A Malonate-Linked Copper (II) Metal Organic Frameworks: X-ray Crystallographic structure

Kalawati Saini
Miranda House, Chemistry Department, University of Delhi, New Delhi-110007
Corresponding Author Email: kalawati.saini@mirandahouse.ac.in

Abstract

The new copper (II) extended metal organic frameworks (MOFs) with malonic (mal = malonate) have been synthesized using electrochemical route and characterized by SXRD, PXRD ,TGA/DTA, and infrared spectroscopy. MOFs are crystalline solids in which the metal ions and or ligands are assembled infinitely resulting in one, two or three-dimensional networks having direct metal-ligand coordination. The presence of ammonia and N-Cetyl tri methyl ammonium bromide plays important role in the structure of abovementioned MOFs during electrochemical synthesis. The growth of the solids and the polymorphs are interpreted in term of self assembly between a reasonable soluble molecules reacting in the supramoleculer reaction along the mechanistic approach proposed by Ramanan and Whittingham during the nucleation of MOFs crystals.

metal, ligands , polymorphs , supramoleculer, crystal.

1. Introduction

Metal centers play a key role in the molecular recognition process in extended materials and biological systems. In this context, copper has attracted considerable attention mainly due to their attractive magnetic properties, photoluminescence, novel structural features and biological relevance involving the binuclear "CuA" site in cytochrome oxidases and related model compounds. Since the last decade enormous research efforts have been diverted towards the synthesis and application of MOFs. Structural correlation with magnetic and Photocatalytic activity has been studied for hexanuclear copper-based secondary building unit[1]. Ultraporous, Water Stable, and Zirconium-Based Metal–Organic Frameworks with ftw Topology have been studied by Pravas Deria[2].

The complexes of transition metal ions with dicarboxylate ligand have been extensively studied in the field of molecular magnetism and in material chemistry on account of its promising application in the area of technology since it exhibit a variety of chelating abilities resulting in dinuclear ,tetranuclear ,1D,2D and 3D networks. A few of these systems are also useful in material chemistry for solvent exchange due to the presence of open frameworks in their molecular structure. Among the different dicarboxylates, major work has been done with oxalate, coordinating in a bisbidentate chelating fashion. The crystal structure and low temperature magnetic behaviour of 1D chains of Cu (II) with oxalate as one of the bridging ligands have been reported in the literatrue.

Recently, many functional supramolecular architectures have been designed and synthesized in the scope of crystal engineering via the coordination force, hydrogen bonding and other intermolecular interactions[3-8]. Although, there are still many challenges to understand these tailor-made molecular materials, because the structural control is often received by the delicate and noncovalent nature of the weak interactions[9]. The crystal engineering can be further interesting when the starting reactants comprise two or more distinct molecular / ionic component and the hybrid nature of the resultant materials expands the range of their potential applications.

During the last three decades, particular guidelines for manipulating the molecular assembly into the prescribed crystalline

architecture via hydrogen bonding continue to be attractive [10-11]. In the literature many MOFs have been synthesized in which the charge-assisted hydrogen bonds are strong, directional as well as compliant in nature. In this context, coordination complexes with peripheral hydrogen-bonded participant have many challenges[12-17], because the metal ions may also coordinate with the electronegative donar that are favourable hydrogen bonding sites. The structural connection of these complexes is discussed from the facets of metal ions and water components, as well as the binding diversification of malonate.

The Metal-organic coordination polymers (MCP) or Metal Organic Frameworks (MOFs) have been classified as solids in which the metal ions and organic ligands, self-assemble infinitely leading to one-, two- and three-dimensional networks, having direct metal ligand coordination at least along any one of the dimensions. The ligand must have at least one carbon atom between the donor atoms[18]. It is the bridging organic ligands which allow for the large diversity in the topologies and possible properties of the metal-organic coordination networks. While the ability of metals to exist in multiple oxidation states exhibiting different coordination geometries and the multidentate nature of organic ligands dictates the dimensionality and directionality of the metal-ligand coordinate covalent bonds; flexibility, functionality and chirality in the MOFs is imposed by the nature of the ligand.

MOFs are formed by self-assembly of metal ions and organic ligands wherein neutral molecules or ions present in the medium recognize each other and communicate in terms of specific bonding. Apart from the strong electrostatic forces operating between the various ions, nonbonding interactions also influence the organization of these species. It is well known that metal ions that are susceptible for hydrolysis in a solution can be stabilized by the formation of complexes using suitable organic amines or acids. Though this strategy is widely employed to assemble MCP, no one has recognized the true primary building blocks that are crucial for the overall structural organization. In this context the paper of Ramanan and Whittingham is significant wherein they have demonstrated the occurrence of several neutral MOFs in terms of chemical events that precede the nucleation of a particular crystal[19]. As soon as a metal salt is dissolved in water or a nonaqueous solvent, a soluble metal complex is initially formed. The most important driving forces involved in the self-assembly of metal ions and ligands involves spontaneous ordered aggregation of their soluble molecular precursors. The aggregation and there after condensation of the molecular species to form a particular solid is dictated by

The ligands used in the construction of coordination polymers have to bridge between metal ions. This requires usually multidentate ligands with two or more donor atoms. Such *bridging* ligands are called di-, tri-, tetratopic depending on the number of donor atoms of special importance are *rigid* bridging ligands since they allow for a certain control of the steric consequences in the assembly process. The diversity of organic components is, of course, the basis for the variety in structural topologies. By carefully selecting the organic ligand one also aims to tune the physical properties and, thus, realize various applications, such as catalysis, electrical conductivity, luminescence, magnetism, non-linear optics or zeolitic behaviour[20-24]. Generally, *nitrogen-* and *oxygen-donor* ligands feature prominently in the construction of coordination polymers. Conventionally framework solids are prepared through reactions proceeding at high temperatures leading to thermodynamically stable compact structures. Since the presence of a liquid phase, usually an aqueous solution, favours the diffusion of small ionic or molecular species, low temperature chemical routes such as co-precipitation, sol-gel, solution evaporation, hydrothermal syntheses, etc. have been employed to obtain metastable materials with open structures. One of the main advantages of wet chemical methods is that weak interactions (hydrogen bonds, CH…., π….π interactions etc.) are not broken at low temperature. They are involved in the self-assembly of molecular precursors and can play an important role during the formation of the MOFs.

Long-range ordering of paramagnetic metal ions in coordination polymers causes them to be suitable candidates for molecule-based magnets. Multidentate, closed shell organic ligands, which are typically used in coordination polymers, give mostly rise to only weak magnetic interactions. In order to achieve a strong coupling between the metal centers with their unpaired electrons, short oxo, cyano or azido bridges are needed.

It is crucial to understand the formation of a particular solid in terms of the molecular precursors involved in the self-assembly. In order to reduce the interference of other ions instead of using copper salts such as in solution evaporation method, the synthetic route employed herein, is electrochemical. Therefore, while varying the applied potential one can control the concentration of copper ions in solution, the growth of MOFs can be controlled by varying the concentration of ligand in the solution. The present paper is thus an attempt to synthesize single phasic MOFs based on copper and understand their formation in terms of the reacting molecular precursors via electrochemical route. Besides the morphology of the product (powder or single crystals) can be altered with variation in experimental parameters such as applied external potential, concentration of reaction mixture, solvent and scan rate (mV/s).

2.0 Experimental

2.1 Materials

Copper electrode (99.99% pure) was taken as the anode and platinum wire (99.99 % pure) was taken as the counter electrode. The electrodes were dipped in an aqueous solution of the organic ligand of known molarity. Analytical grade (A.R.) of malonic was used as received commercially. Potential was applied for a fixed time interval using a potentiostat (Potentioscan Wenking Model POS 73) and potential applier. Single crystals were obtained by slow evaporation of the resultant clear solution at room temperature. Table 1 summarizes the experimental conditions for the synthesis of MOFs.

2.2 Characterization

Room-temperature powder X-ray diffraction (PXRD) data were collected with a Bruker D8 Advance diffractometer using Ni-filtered Cu-*K*α radiation. Data were collected with a step size of 0.05° and a count time of 1 s per step over the range 2° <2θ <60°. Single crystal diffraction (SXRD) studies were carried out on a Bruker AXS SMART Apex CCD diffractometer with a

Table 1. Experimental conditions for the synthesis of MOFs

Sample Code	Anode	Cathode	Reaction Medium	Applied Potential (V)	Duration (Hours)	Remarks
KS1	copper	platinum	20 mL of 0.1 M malonic acid with 3.145 mmol of Liquor Ammonia Solution	12.5	12	Blue crystals of $[(NH_4)_2Cu(mal)_2]$
KS2	copper	platinum	20 mL of 0.1M malonic acid with 3.145 m mol of N-Cetyl tri-methyl ammonium Bromide	12.5	12	Better crystals of $[Cu(mal)_2(H_2O)(OH)]$ $[Cu(mal)(OH)_4]$

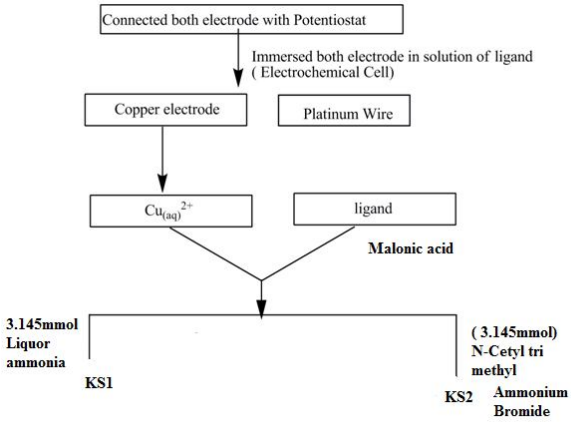
Mo Kα (0.71073Å) sealed tube at 28°C. Semi-emprical absorption corrections were applied using SADABS and SHELXTL for space group and structure determination and refinements. There was no evidence of crystal decay during data collection. The program SAINT was used for integration of the diffraction profiles. The non-hydrogen atoms were modelled with anisotropic displacement parameters and refined by full-matrix least-squares methods on F2 .Metal centers were located first and then remaining atoms were deduced from subsequent difference Fourier map. Hydrogen atoms were located using geometrical constraints. All atoms except H were refined anisotropically. The least-squares refinement cycles on F^2 was performed until the model converged. Thermogravimetric analysis (TGA) was carried out using Perkin–Elmer TGA7 and DTA7 system on well ground samples in flowing nitrogen atmosphere from 40-940°C at a scanning rate of 10 °C min^{-1}. These studies were carried out to analyze the thermal stability of the obtained products and to ascertain the temperature at which the evolution of the organic moiety occurred. Fourier Transformed Infra Red (FTIR) spectra were recorded on a Nicolet 5DX spectrophotometer with pressed KBr pellets in the range 4000 to 400cm^{-1}.

3.0 Results and Discussion

The synthesis of copper based MOFs was carried out by using malonic acid as this has more than one donor sites and can chelate with copper. When copper electrode is taken as anode it oxidizes to give cupric ions in solution. These ions may undergo further hydrolysis to form soluble molecular precursors. On increasing the reaction time, the color of the solution changes from colorless to intense blue indicating complexation of the ligand with copper.

3.1 MOFs of Copper with Malonic acid

Oxidation of Cu electrode and followed by complexation with ligand at room temperature produced intense blue coloured solution. The resultant solution was left undisturbed at room temperature and blue crystals were obtained after a few days (refer scheme 1). While direct electrochemical synthesis using ligand and copper electrode did not yield any product in the case of only with malonic acid. Therefore, a small amount of NH_3 solution (3.145 mM) in set-1 and N-Cetyle trimethyl ammonium bromide in set-2 was added to enhance the ionization of the malonic acid and thereby facilitate the complexation with the metal.



Scheme 1. Scheme showing the results obtained using the electrochemical route.

$[(NH_4)_2\ Cu(mal)_2]$, KS1

0.208 g of malonic acid (0.1M) was dissolved in 20 ml of water and 3.145mM of liquor ammonia was added. Copper electrode was taken as the anode and Pt was taken as the reference electrode. External potential (12.5 V) was applied for 12 hours. A clear blue solution was obtained. Blue block and cube-like crystals of $[(NH_4)_2Cu(mal)_2]$ were grown by slow evaporation of the resulting clear solution at room temperature.

Crystal Structure of $[(NH_4)_2Cu(mal)_2]$

The new copper (II) extended metal organic framework $(NH_4)_2\ [(Cu\ (mal)_2]$

(mal = malonate) has been synthesized via electrochemical route route and characterized by TGA/DTA, PXRD, and infrared spectroscopy. The crystal structure of the complex $(NH_4)_2\ [(Cu\ (mal)_2]$ was studied by the single crystal XRD. X-ray crystallographic study reveals that the metal coordination spheres in KS1 is similar within a monomeric building block $[M(mal)_2]^{-2}$, which is charge-balanced by the cationic diammonium component. This compound

crystallizes in the orthorhombic space group : f d d 2 with a = 13.925(5) A^{o} , b = 16. 524(6) A^{o}, c= 9.137(3) A^{o} , V= 2102.39, Z= 8 and chemical formula $C_6 H_{12}Cu_1N_2O_8$. Every copper has a distorted octahedral centre, formed by four oxygen atoms (from two bidentate malonate ligands) in the equatorial sites. The two axial positions are occupied by two oxygens from two different malonate ligands forming a distorted octahedral geometry around copper atom and extending into 2-D sheets (Figure 1b). Thus the structure consists of copper malonate complexes extending into 2-D sheets through oxygen atoms. These sheets are inter crossed through axial oxygen in zigzag manner and forms 3-D open framework (Figure 1,2,11,12 and 13). Four oxygen atoms from two bidentate malonate ligands and remaining two oxygens from two different malonate ligands forming a distorted octahedral geometry around copper atom and extending into 2-D sheets (Figure 2, view along c axis and Figure 10). One oxygen atom of each malonate remains free. Ammonium ions joins with copper malonate framework by electrostatic attraction. It also participates in hydrogen bonding with oxygen of malonate. In this way the copper malonate change in to complicated 3D structure (Figure 4).

We have made an attempt to understand the formation of the solid based on Ramanan and Whittingham's hypothesis as shown in Figure 3. The crystallographic details of **KS1** are given in Table 2. The bond distances and bond angles are given Table 3.

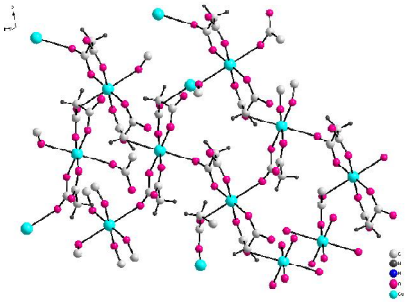


Figure1. Crystal structure of [$(NH_4)_2(mal)_2$], $(^{+}NH_4)_2$ ions are omitted from crystal structure for simplicity.

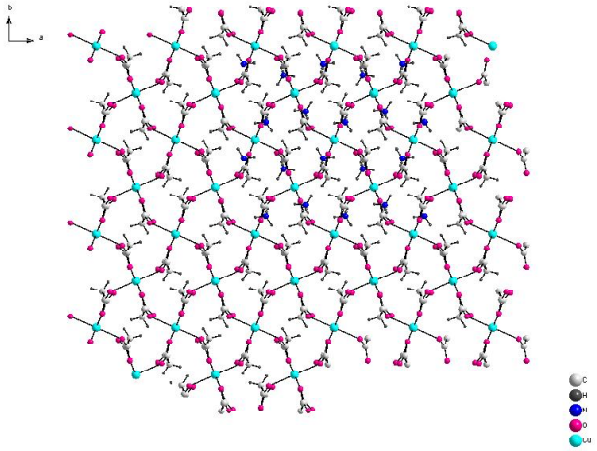
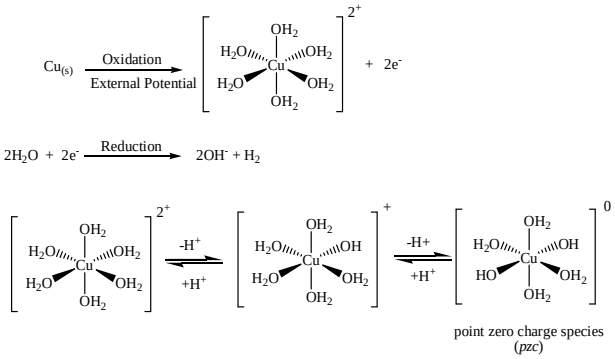


Figure 2.The figure shows 3-D framework formed by 2-D copper malonate sheets, Zigzag chains formed through the coordination of malonate-oxygen atoms (View along c axis) .



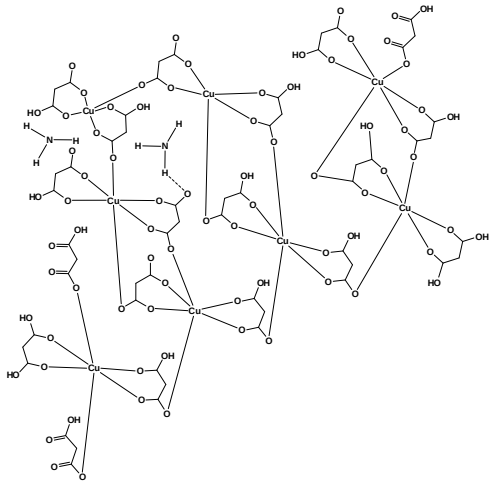


Figure 3. Soluble cupric tetra aqua dihydroxyl condense with malonate ions to form 2D sheets which are further linked by ammonium ions by hydrogen bonding.

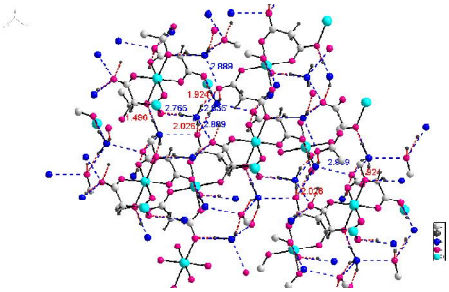


Figure 4. Crystal structure of [$(NH_4)_2(mal)_2$], **KS1** Showing hydrogen bonding (-N-H.....O) , Hydrgen bonding varies 2.026-2.889 Å

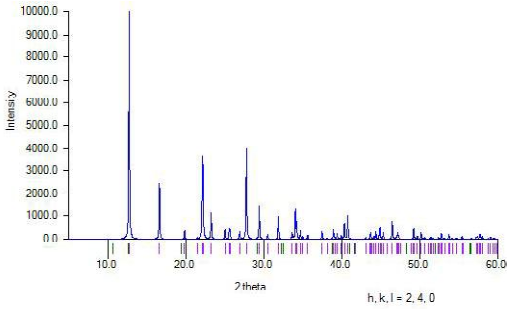


Figure 5. Powder x-ray diffraction of single crystal of [$(NH_4)_2(mal)_2$] ,**KS1**generated from CIF after opening in mercury software

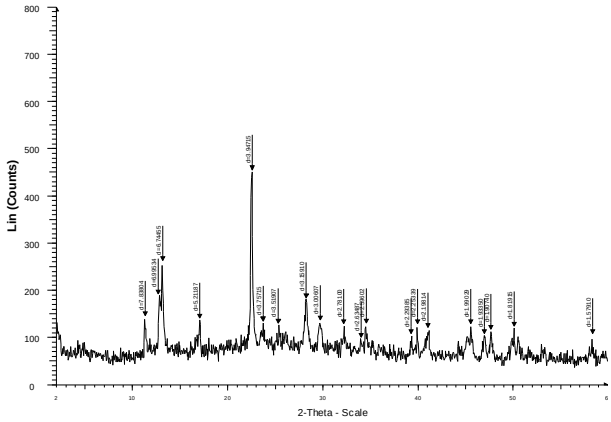


Figure 6.Powder x-ray diffraction of of [$(NH_4)_2(mal)_2$] **KS1**

The phase purity of the above solid has been ascertained using PXRD. The PXRD of single crystal has been generated with submitted CIF (See CIF No. 688412). The PXRD pattern of single crystal of **KS1** is given in Figure 5.This pattern matches well with the PXRD pattern of the bulk material (Figure 6). The FTIR spectrum of **KS1** shows a strong band in the region 646.24-735.50 cm^{-1} that can be attributed to ν (Cu–O) vibration (Figure 7). The bands at 1175.56 cm^{-1},

Table 2. The Instrument and crystallographic experimental details of diammonium copper dimalonate [$(NH4)_2Cu(mal)_2$], **KS1**,

Diffractometer	Bruker AXS SMART Apex CCD		Crystal size, mm^3 0.204x 0.148×0.102
Empirical formula	$C_6 H_{12} Cu N_2 O_8$	Formula weight	303.73
Crystal system	Orthorhombic	Space group	F d d 2
Unit cell dimensions	a = 13.925(5) Å	Volume, Å	2102.4(13)
	b = 16.524(6) Å	Z	8
	c = 9.137(3) Å	$D_{cal,}$ g cm^{-3}	1.919
		F(000)	1240
μ (Mo- Kα), mm^{-1}	2.114	Reflections used	3089
Reflection collected	4673	Parameters refined	94
Reflections with *I*>2σ(*I*)	916	*R* for *I*>2σ(*I*)	0.0443
R (all data)	0.0447	*wR* for *I*>2σ(*I*)	0.1079
w	1/[\s^2^(Fo^2^)+(0.0412P)^2^+33.0407P] where P=(Fo^2^+2Fc^2^)/3'	R-Factor(%)	4.43
Goodness-of-fit on F	1.182	CCDC deposition no.	688412
Program	SHELXL-97		

Table 3. Bond distances and bond angles of copper malonate [$(NH4)_2Cu(mal)_2$], **KS1**,

Bond distances (Å)	Bond angles (°)
C1- O1 1.278	O1-C1- O5 120.4
C1- O5 1.282	O1- C1- C2 120.9
C1- C2 1.502	O5- C1- C2 118.7
C2- C3 1.533	C1- C2 -C3 116.6
C2 -H2A 0.9700	C1- C2 -H2A 108.2
C2 -H2B 0.9700	C3- C2 -H2A 108.2
C3- O3 1.236	C1 -C2- H2B 108.2
C3-O2 1.252	C3 -C2- H2B 108.2
Cu1 -O1 1.947	H2A -C2- H2B 107.3
Cu1 -O1 1.947	O3 -C3 -O2 123.0
Cu1- O5 2.478	O3- C3- C2 117.4
Cu1- O2 1.967	O2- C3 -C2 119.5
Cu1- O2 1.967	O1- Cu1- O1 86.7
N2 -H1 0.95	O1- Cu1- O2 179.3
N2 -H2 0.98	O1- Cu1- O2 92.62
N2- H3 0.49	O1 -Cu1- O2 92.62
N2 -H4 1.27	O1- Cu1- O2 179.3
	O2- Cu1- O2 88.1
	H1- N2- H2 117.0
	H1- N2- H3 94.0
	H2- N2 -H3 131.0
	H1- N2- H4 111.0
	H2 -N2 -H4 103.0
	H3- N2 -H4 99.0
	C1- O1- Cu1 127.6
	C3- O2 -Cu1 126.9

1898.34-1561.76 cm^{-1}, 2137.02 cm^{-1}, and 2999.82 cm^{-1} are attributed to ν(C-C), ν(C=O), ν(COOH) and ν(C-H) respectively. Thermogravimetric analysis (TGA) of **KS1** reveals that the decomposition of the complex occurs in three consecutive steps, namely, deammoniation, ligand pyrolysis and finally, inorganic residue formation (Figure 8). The deammoniation process occurs in the range 170-200ºC in a single step, which corresponds to the loss of two ammonium ions . The second (280 -380 ºC) and third (380-500 ºC) steps are the pyrolysis of the ligand.The residue of TGA matches with reported powder x-ray pattern of CuO, as shown in figure 9.

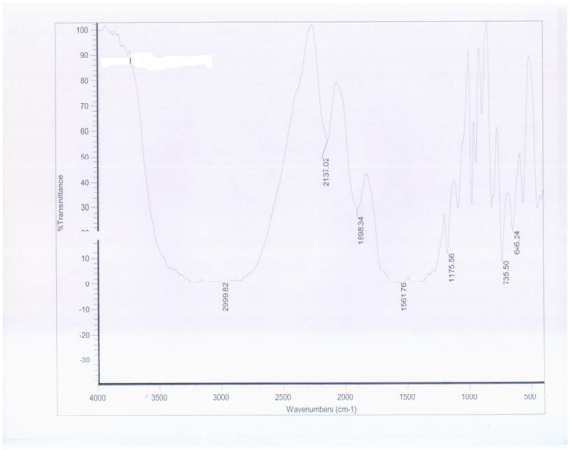


Figure7. FTIR spectrum of [$(NH4)_2$ $Cu(mal)_2$], **KS1**.

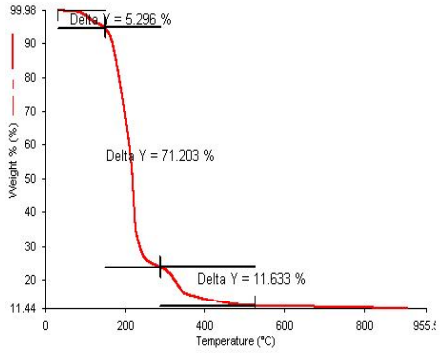


Figure 8. TG normalise curve of diammonium copper malonate(NH4)2[Cu (mal)2],**KS1**

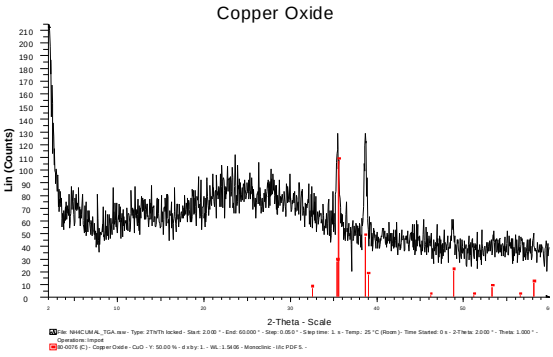


Figure 9.Matched Powder X-Ray Diffraction of TGA residue with PXRD of CuO (JCPDS No.80-0076)

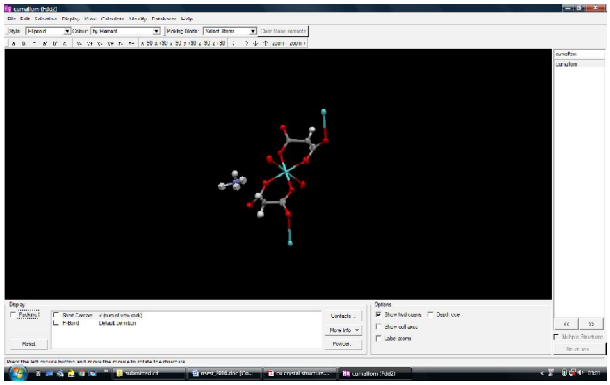


Figure10. Single crystal (Elipsoid model)of [$(NH_4)_2(mal)_2$] ,**KS1**generated from CIF after opening in mercury(C gray,Cu cyan, N blue, O red,H white)

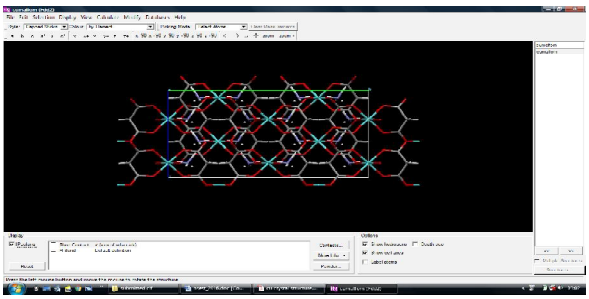


Figure 11. Packed Single crystal (capped sticks model) of [$(NH_4)_2(mal)_2$] ,**KS1**generated from CIF after opening in mercury(C gray,Cu cyan, N blue, O red,H white), View along a axis

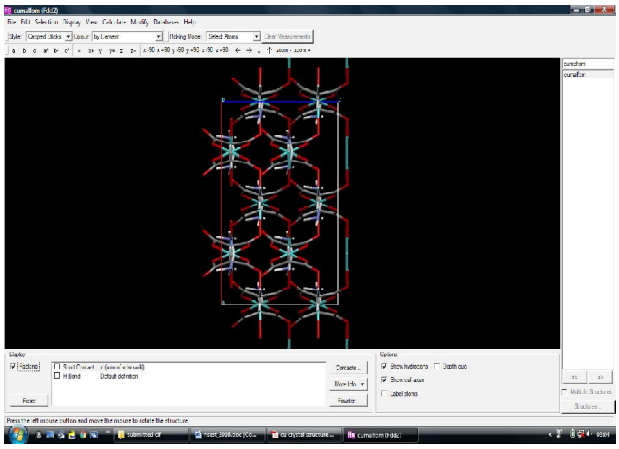


Figure12. Packed Single crystal (capped sticks model)of [$(NH_4)_2(mal)_2$] ,**KS1**generated from CIF after opening in mercury(C gray,Cu cyan, N blue, O red,H white), View along b axis

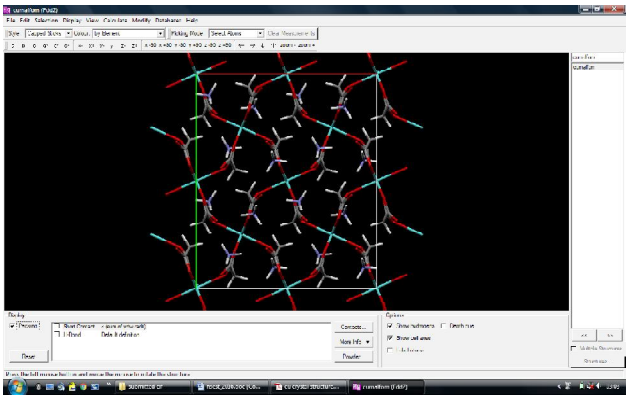


Figure 13. Packed Single crystal (capped sticks model)of [$(NH_4)_2(mal)_2$] ,**KS1**generated from CIF after opening in mercury(C gray, Cu cyan, N blue, O red, H white), View along c axis

$[Cu(mal)_2(H_2O)(OH)]$ $[Cu(mal)(OH)_4]$, KS2

0.208 g of malonic acid (0.1M) was dissolved in 20 ml of water and 3.145mM of N-Cetyl tri methyl ammonium bromide was added. Copper electrode was taken as the anode and Pt was taken as the reference electrode. External potential (12.5 V) was applied for 12 hours. A clear blue solution was obtained. Blue block like crystals of [Cu $(mal)_2(OH)][Cu(mal)(OH)_4]$, were grown by slow evaporation of the resulting clear solution at room temperature.

The new copper (II) discreet metal organic framework $[Cu(mal)_2(H_2O)(OH)]$ $[Cu(mal)(OH)_4]$, **KS2,** where (mal = malonate) has been synthesized via electrochemical route route and characterized by TGA/DTA, PXRD, and infrared spectroscopy. This compound crystallizes in the orthorhombic space group : P b c n with a = 14.895(12) A^o , b = 15.005(12) A^o , c = 12.666(10) A^o , V=2831(4) , Z= 8 and chemical formula $C_6 H_9 Cu_2 O_{14}$.

In this structure two types of copper units are obtained in which one copper atom (Cu1) has distorted pentahedral centre, formed by four water molecules are occupied in equatorial position and having equivalent bond. The fifth oxygen which is occupied axial position coming from malonate ligand (Figure 14 and 15). The another copper (Cu2) has a distorted octahedral centre , formed by four oxygen atoms(from two bidentate

malonate ligands) in the equatorial sites. The two axial positions are occupied by two oxygens from two water molecules forming a distorted octahedral geometry around copper atom (Figure 14 and 15). Thus the structure consists of discreet complexes of copper malonate which does not extend through oxygen atoms as crystal structure of [$(NH_4)_2(mal)_2$], **KS1.** In the structure of **KS2**, the axial one water ligands in the Cu(II) coordination sphere are located without hydrogen atom. However the different coordination mode of the malonate anion towards copper induces different topologies and different MOFs along different crystallographic axis (Figure 16-20). In this structure out of two malonate ligand one malonate has two oxygen atom free while another malonate ligand has one oxygen atom free.

The average M-O distances in the equatorial plane are for **KS1** , Cu1- O1 1.947 Å and Cu1-O2 1.967 Å. The M-O distances in the axial plane is 2.48 Å. But for **KS2** M-O distances in the equatorial plane are Cu1- O9 1.922 Å, Cu1- O10 1.946 Å, Cu1- O12 1.927 Å, Cu1 -O11 1.933 Å, Cu2- O4 1.946 Å, Cu2 -O2 1.948 Å, Cu2- O3 1.949 Å, Cu2- O1 1.956 Å. The M-O distances in one unit in the axial planes are Cu1-O8 2.383 Å and in another unit Cu2 -O14 2.419 Å and Cu2-O13 2.517 Å respectively.

These values are also in good agreement with those observed in the related malonate-containing complexes[25-30]. As for the apical M-O lengths (2.478 Å for KS1 and 2.383 Å, 2.419 Å, 2.517 Å for KS2), they are slightly longer than those of the equatorial M-O bonds. As expected, the Cu (II) ion in KS1 and KS2 shows the typical John-Taller distortion with the significantly longer axial Cu-O distances. The Cu....Cu distance is found to be 5.86 Å for **KS1**.Further details for crystallographic data **KS2** are listed in Table 4. The bond distances and bond angles are given Table 5.

Table 4. Crystal data for copper dimalonate $[Cu(mal)_2(H_2O)_2]$ [$Cu(mal)(OH)_4$], **KS2**,

Diffractometer	Bruker AXS SMART Apex CCD	Crystal size, mm^3	0.508 x 0.264 × 0.178
Empirical formula	$C_6 H_9 Cu_2 O_{14}$	Formula weight	432.23
Crystal system	Orthorhombic	Space group	P b c n
Unit cell dimensions	a = 14.895(12) Å	Volume, Å	2831(4)
	b = 15.005(12) Å	Z	8
	c = 12.666(10) Å	$D_{cal,}$ g cm^{-3}	2.028
	F(000)	720.0	
μ (Mo- Kα), mm^{-1}	3.077	Reflections used	2855
Reflection collected	2320	Parameters refined	204
Reflections with $I>2\sigma(I)$	1636	*R* for $I>2\sigma(I)$	0.0578
R (all data)	0.0809	*wR* for $I>2\sigma(I)$	0.1507
w	1/[\s^2^(Fo^2^)+(0.1133P)^2^+0.0000P] where P=(Fo^2^+2Fc^2^)/3''	R-Factor(%)	z5.78
Goodness-of-fit on F	0.982	Reflection number total	2497
Program	SHELXL-97	CCDC deposition no.	704401

Table 5. Crystal data for copper dimalonate $[Cu(mal)_2(H_2O)_2]$ [$Cu(mal)(OH)_4$], **KS2**,

Bond distances (Å)	Bond angles (°)
Cu1- O9 1.922	O9 -Cu1- O12 90.04
Cu1- O12 1.927	O9- Cu1- O11 174.2
Cu1- O11 1.933	O12- Cu1- O11 89.12
Cu1- O10 1.946	O9 -Cu1- O10 90.44
Cu1- O8 2.383	O12 -Cu1- O10 173.46
Cu2- O4 1.946	O11- Cu1- O10 89.76
Cu2 -O2 1.948	O9 -Cu1- O8 95.82
Cu2 -O3 1.949	O12- Cu1- O8 91.09
Cu2 -O1 1.956	O11- Cu1- O8 89.88
Cu2 -O14 2.419	O10 -Cu1- O8 95.35
Cu2-O13 2.517	O4- Cu2- O2 179.22
O3 -C3 1.270	O4 -Cu2- O3 89.13
O2 -C1 1.283	O2- Cu2- O3 91.63
O4- C4 1.280	O4- Cu2- O1 91.06
O1- C6 1.277	O2- Cu2 -O1 88.18
O8- C6 1.251	O3- Cu2 -O1 179.32
O11- H11 0.8200	O4- Cu2- O14 88.25
O9 -H9 0.8200	O2- Cu2- O14 91.91
C3 -O6 1.244	O3 -Cu2 -O14 91.78
C3- C2 1.511	O1- Cu2- O14 88.87
O12- H12 0.8200	C3 -O3- Cu2 126.5
O5- C1 1.235	C1 -O2- Cu2 125.8
O10- H10 0.8200	C4 -O4 -Cu2 126.0
C6 -C5 1.505	C6 -O1 -Cu2 125.9
C1- C2 1.507	C6 -O8 -Cu1 121.2
O14 -H14 0.8200	Cu1 -O11- H11 109.5
O7- C4 1.234	Cu1- O9- H9 109.5
C4- C5 1.512	O6 -C3- O3 122.9
C5- H5A 0.9700	O6- C3- C2 117.7
C5 -H5B 0.9700	O3 -C3 -C2 119.4
C2- H2A 0.9700	Cu1- O12 -H12 109.5
C2- H2B 0.9700	Cu1- O10- H10 109.5
	O8- C6- O1 121.5
	O8- C6- C5 118.7
	O1- C6- C5 119.7
	O5 -C1- O2 121.5
	O5 -C1- C2 118.9
	O2 -C1- C2 119.5
	Cu2- O14- H14 109.5
	O7 -C4 -O4 122.9
	O7- C4- C5 117.6
	O4- C4- C5 119.4
	C6- C5 -C4 119.1
	C6- C5- H5A 107.5
	C4- C5 -H5A 107.5
	C6 -C5- H5B 107.5
	C4 -C5- H5B 107.5
	H5A- C5 -H5B 107.0
	C1- C2 -C3 119.8
	C1 C2 H2A 107.4
	C3 C2 H2A 107.4
	C1 C2 H2B 107.4
	C3 C2 H2B 107.4
	H2A C2 H2B 106.9

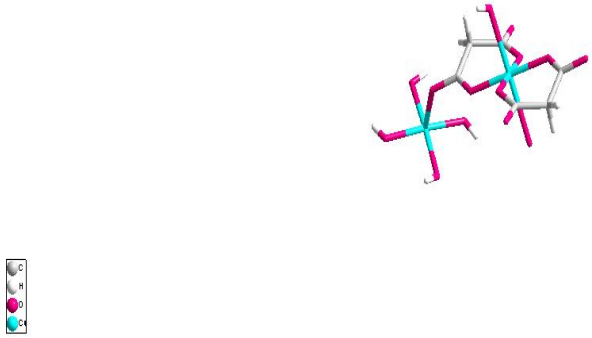


Figure14. Crystal structure of $[Cu(mal)_2(H_2O)(OH)][Cu(mal)(OH)_4]$, **KS2** (Stick model)

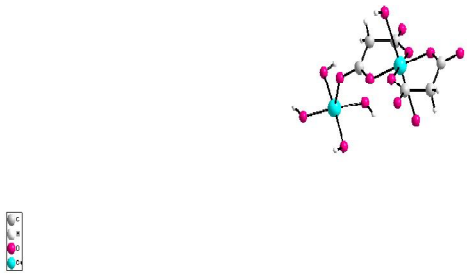


Figure 15. Single crystal of $[Cu(mal)_2(H_2O)(OH)][Cu(mal)(OH)_4]$,**KS2**

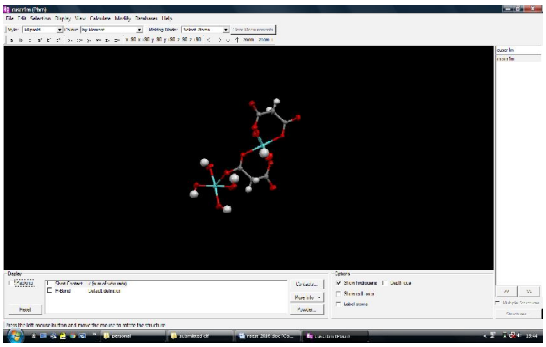


Figure 16. Single crystal (Elipsoid model)of $[Cu(mal)_2(H_2O)(OH)][Cu(mal)(OH)_4]$, **KS2** generated from CIF after opening in mercury(C gray,Cu cyan, O red,H white)

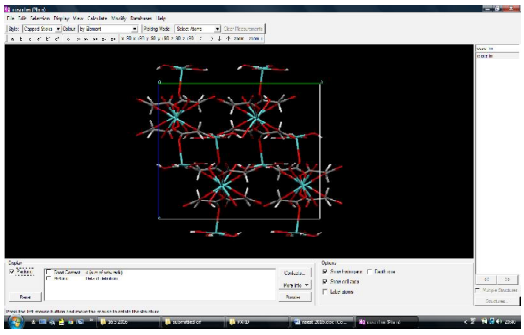


Figure 17. Single crystal (Capped stick model)of $[Cu(mal)_2(H_2O)(OH)][Cu(mal)(OH)_4]$, **KS2** generated from CIF after opening in mercury(C gray,Cu cyan, O red,H white), View along a axis

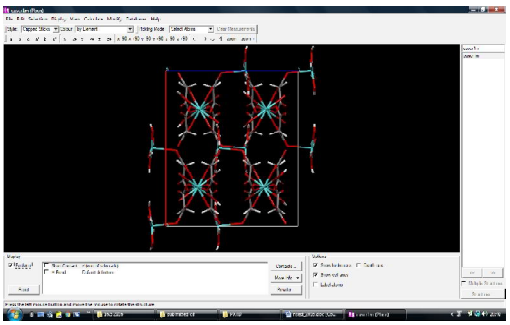


Figure 18. Single crystal (Capped stick model)of $[Cu(mal)_2(H_2O)(OH)][Cu(mal)(OH)_4]$, **KS2** generated from CIF after opening in mercury(C gray,Cu cyan, O red,H white),view along b axis

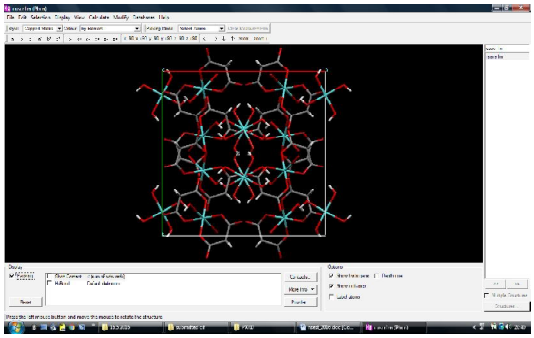


Figure 19. Single crystal (Capped stick model)of $[Cu(mal)_2(H_2O)(OH)][Cu(mal)(OH)_4]$, **KS2** generated from CIF after opening in mercury(C gray,Cu cyan, O red,H white),View along c axis.

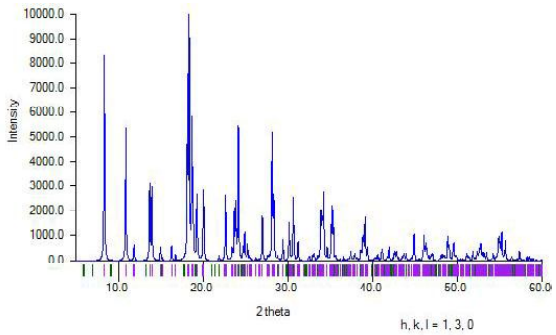


Figure 20.Powder x-ray diffraction of single crystal of $[Cu(mal)_2(H_2O)(OH)][Cu(mal)(OH)_4]$, **KS2**generated from CIF after opening in mercury

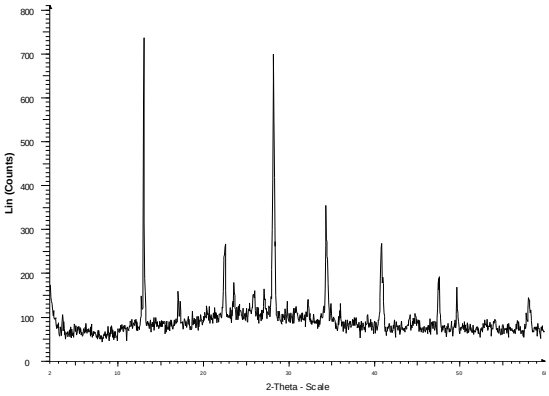


Figure 21.Powder x-ray diffraction of $[Cu(mal)_2(H_2O)(OH)][Cu(mal)(OH)_4]$, **KS2**

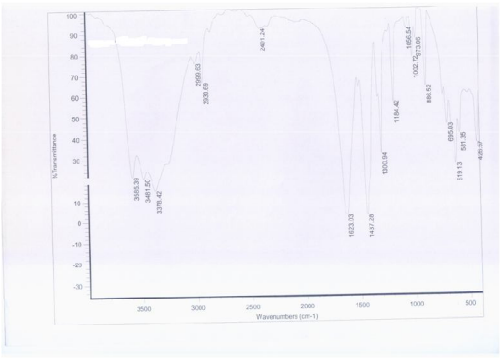


Figure 22. FTIR spectrum of [Cu $(mal)_2(H_2O)(OH)][Cu(mal)(OH)_4]$,**KS2**.

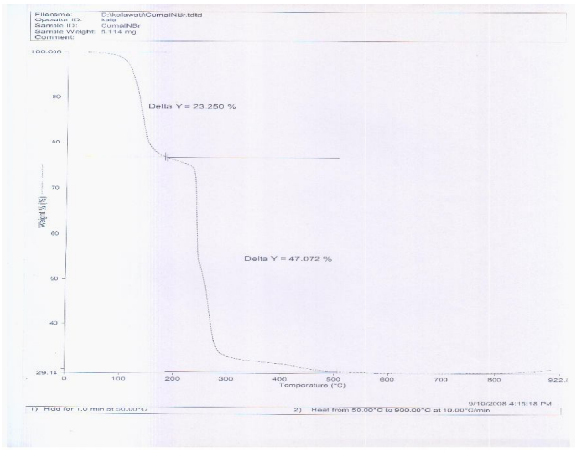


Figure 23. TGA of copper malonate $[Cu(mal)_2(H_2O)_2]$ $[Cu(mal)(OH)_4]$, **KS2**

The phase purity of the above solid has been ascertained using PXRD. The PXRD of single crystal has been generated with submitted CIF (See CIF No. 704401). The PXRD pattern of single crystal of **KS1** is given in Figure 20. This pattern matches well with the PXRD pattern of the bulk material (Figure 21).

The FTIR spectrum (Figure 22) of **KS2** shows a strong band in the region 426.57-581.35 cm^{-1} that can be attributed to ν (Cu–O) vibrations. The bands at 1300.94-1184.42 cm^{-1}, 1623.03-1437.28 cm^{-1}, 2401.04 cm^{-1} , 2999.63-2930.69 cm^{-1} and 3378.42-3585.39 cm^{-1} are attributed to ν(C-C), ν(C=O), ν(COOH) ν(C-H) and ν(O-H) respectively. Thermogravimetric analysis of **KS2** (Figure 23) reveals that the decomposition of the complex occurs in three consecutive steps, namely, dehydroxylation, ligand pyrolysis and finally, inorganic residue formation. The dehydroxylation process occurs in the range 100-200ºC in a single step, which corresponds to the loss of five hydroxyl ions . The second (200 - 500 ºC) step is the pyrolysis of the ligand.

4.0 Conclusion

This work has been an attempt towards the understanding of the subtle factors that regulate the organization of solids. By careful selection of appropriate ligands, we were able to predict the various combinations possible through coordination, thereby, controlling the pore size of the framework solid. The bidentate malonate ligands resulted in 3D framework structures for KS1, while the same bidentate ligand produced discreet complex, which was connected through weak interactions (H- bonding) resulted into 2D and 3D structures respectively. Thus presence of ammonia and N-Cetyl tri methyl ammonium bromide plays important role in the structure of abovementioned MOFs during electrochemical synthesis. The repeating units of $[(NH_4)_2$ (Cu ($mal)_2]$ contains two types of 4+ 2 coordination , in which each copper is surrounded by four oxygen of malonate anion and two oxygen of water molecules.

It was observed that with the increase in external potential, the rate of oxidation of metal increased. The complexation rate increased, with the formation of powder precipitate. But at an optimum applied potential, controlled oxidation of metal electrode took place, resulting in the formation of soluble metal – ligand complex. On standing and slow evaporation at room temperature, fine crystals of the complex were obtained. We have presented the explanation for the different morphology on the basis of the proposed pathway of structural organization by Ramanan and Whittingham. The solvated metal ions form the starting point for solid formation. Subsequently the ligand molecules attach themselves to the central metal ion, forming a template for crystal growth. Dehydration on slow evaporation leads to the formation of the solid.

In the case of malonic acids (weak aliphatic acids), increase in external potential had no effect on complexation due to extremely weak ionization of the ligand molecules. Dramatic

change took place when 3.145mmol of liquor ammonia and N-Cetly tri methyl ammonium bromide were added. Complexation took place effectively at12.5 V in both sets of experiment.

By understanding the role of anode, ligand, applied external potential and content and concentration of reaction mixture in solid organization, we believe that the electrochemical route for MOF synthesis holds lot of promises for future explorations.

Acknowledgement

Authors wish to thank Professor A. Ramanan, Department of Chemistry, Indian Institute of Technology Delhi for providing guidance and also thank to Indian Institute of Technology for providing facility for SXRD,PXRD,TGA and FTIR analysis. The Author also thank Council of Scientific & Industrial Research (CSIR), CSIR Complex, Library Avenue, Pusa, New Delhi - 110 012 India, for providing fund for this work.

References:

1. S. Bala, S. Bhattacharya, A. Goswami, A. Adhikary, S. Konar, and R. Mondal, *Cryst. Growth Des.* ***14*** **(12)**, 6391 (2014).
2. P. Deria *etal* , *J. Am. Chem. Soc.***137** (40), 13183 (2015).
3. G.M.J. Schmidt, *Pure Appl. Chem*. **27**, 647 (1971); (b) G.R. Deshraju, Crystal Engineering :The Design of Organic Solids, Elsevier ,Amsterdam,1989.
4. C.Janiak, *Dalton Trans.* (2003) 2781.
5. M. Nishio, *Cryst Eng Comm* **6**, 130 (2004).
6. G.R. Desiraju .*J.Mol.Struct.* **656**, 5 (2003).
7. B.Moulton, M.J.Zaworotko, Chem.Rev.101,1629 (2001).
8. (a) T. Steiner, Angew.Chem.,Int.Ed. **41**, 48 (2002) (b) G.A.Jeffrey, W. Saenger, Hydrogen Bonding in Biological Structure, Springer, Berlin, 1991.
9. K.T. Holman, A.M.Pivovar, J.A. Swift, M.D.Ward, Acc. Chem.Res.**34** ,107 (2001).
10. (a)A.M. Beatty, Coord. Chem. Rev. **246**,131 (2003); (b) C.V.K Sharma, *Cryst.Growth Des*. **2** 465 (2002) ; (c) C.B.Aakeroy, D.J.Salmon. Cryst. Eng. Comm. **7**, 439 (2005).
11. M.D. Ward, *Chem. Commun.* 5838 (2005).
12. M.W. Hosseini, *Acc. Chem. Res* **38**, 313 (2005).
13. A.D. Burrows, R.W. Harrington, M.F. Mahon,S.J.Teat,*Cryst. Growth Des.* **4** 813 (2004).
14. A.K. Ghosh, A.D. Jana, D. Ghoshal, G. Mostafa, N.R. Chaudhari, *Cryst. Growth Des.* **6**, 701 (2006).
15. A.M. Beatty, B. A. Helfrich, G.A. Hogan, B.A. Reed, *Cryst. Growth Des*. **6**,122 (2006).
16. P.D. Beer, P. A. Gale, *Angew Chem., Int. Ed.* **40**, 486 (2001).
17. M. Du, C. P. Li, X. J. Zhao, *Cryst. Eng. Comm*. **8**, 552 (2006).
18. J. Christoph, Dalton Trans. 2781 (2003).
19. A. Ramanan and M. S. Whittingham, Cryst. Growth Des. 6, 2419 (2006).
20. H. Shirakawa, Angew. Chem. Int. Ed. Engl. 40, 2574 (2001).
21. M. Eddaoudi, D. B. Moler, H. Li, B. Chen, T. M. Reineke, M. O. Kee and O. M. Yaghi, Acc. Chem. Res., 34, 319 (2001).
22. C. T. Chen and K. S. Suslick, Coord. Chem. Rev. 128, 293 (1993).
23. M. Fujita, Y. J. Kwon, S. Washizu and K. Ogura, J. Am. Chem. Soc. 116, 1151 (1994) .
24. J. Y. Lu, Coord. Chem. Rev. 246, 32 (2003).
25. K.R. Butler, M.R. Snow, J. Chem.Soc. Dalton Trans. 259, (1976).
26. C. Ruiz-Perez, J. Sanchiz, M. Hernandez-Molina, F. Lloret, M. Julve, Inorg. Chim. Acta ,298, 245 (2000).
27. C. Ruiz-Perez, J. Sanchiz, M. Hernandez-Molina, F. Lloret, M. Julve, Inorg. Chim. Acta ,39 , 1363 (2000).
28. J. Sanchiz, Y. Rodroguez-Martin, C. Ruiz-Perez, A. Mederos, F. Lloret, M.Julve, New J. Chem. 26, 1624 (2002).
29. S. Sain, T.K. Maji, G. Mostafa, T. H. Lu, N.R. Chanduri, New J. Chem. 27, 185 (2003).
30. F. S. Delgado, J. Sanchiz, C. Ruiz-Perez, F. Lloret, M. Julve, Inorg. Chem. 42, 5938 (2003).